DOI 10.1007/s11182-015-0575-9

Russian Physics Journal, Vol. 58, No. 6, October, 2015 (Russian Original No. 6, June, 2015)

SPECIAL FEATURES OF FRACTURE OF A SOLID-STATE TITANIUM ALLOY – NICKEL – STAINLESS STEEL JOINT

R. G. Khazgaliev,[1] M. Kh. Mukhametrakhimov,[1] M. F. Imaev,[1,2] R. U. Shayakhmetov,[1] and R. R. Mulyukov[1,2]

UDC 621.791.18, 621.7.019.4

Microstructure, nanohardness, and special features of fracture of three-phase titanium alloy and stainless steel joint through a nanostructural nickel foil are investigated. Uniformly distributed microcracks are observed in Ti_2Ni *and* TiN_3 *layers joined at temperatures above T = 700°C, whereas no microcracks are observed in the* TiNi *layer. This suggests that the reason for microcracking is an anomalously large change in the linear expansion coefficient of the* TiNi *layer during austenitic-martensitic transformation. Specimens subjected to mechanical tests at T = 20°C are fractured along different layers of the material, namely, in the central part of the specimen they are fractured along the* Ti_2Ti/TiNi *interface, whereas at the edge they are fractured along the* TiNi/$TiNi_3$ *interface.*

Keywords: pressure welding, welding of dissimilar materials, microcracks, fracture.

INTRODUCTION

The development of modern technical devices, in particular, steam generators and heat exchangers of nuclear power plants calls for the manufacture of reliable joints of titanium alloys with other materials. Fusion welding is unreliable, and joining with fastening elements makes the construction heavier. Elimination of the fastening elements will allow one not only to decrease the weight and size of important construction units, but also to implement radically new design solutions. The most common problem is to join titanium alloys with steel and heat resistant nickel alloys. Solid phase welding is a perspective method of joining of these materials. However, direct joint of titanium alloys with these materials is not always possible due to the formation of brittle phases at the interface. For example, the solid phase joint of the titanium alloy with the stainless steel is accompanied by the formation of brittle Fe–Cr–Ti and Fe–Ti based intermetallic phases and by residual stresses caused by different thermal expansion coefficients (TECs) of the materials being joined [1]. One of the methods of solving this problem is the use of a nickel gasket [2]. The intermetallic compounds are not formed at the steel – nickel alloy interface, whereas Ti_2Ni, TiNi, and $TiNi_3$ intermetallic compounds are formed in the titanium alloy – nickel contact. The welding regime is of great importance when the nickel gasket is used. For example, in [1–4] the titanium alloy and steel were joined through a nickel interlayer at high temperatures $T = 850$–950°C. As a result, the brittle Fe–Ti intermetallic compounds were formed even at the nickel–steel interface due to fast diffusion of titanium, which significantly reduced the hardness of specimen joints. To prevent diffusion of titanium into steel, the temperature or joining time must be decreased. The mechanical properties of the specimens obtained by joining of the titanium alloy with the stainless steel through the nanocrystalline nickel layer at temperatures $T = 650$–750°C were investigated in [5]. The intermetallic Fe–Ti compounds were not formed at these temperatures, and the hardness of the joint was higher than after joining at temperatures $T = 850$–950°C.

[1]Institute for Metals Superplasticity Problems of the Russian Academy of Sciences, Ufa, Russia, e-mail: sloth-usatu@mail.ru; msia@mail.ru; marcel@imsp.ru; ruslanshay@mail.ru; radik@imsp.ru; [2]Bashkir State University, Ufa, Russia. Translated from Izvestiya Vysshikh Uchebnykh Zavedenii, Fizika, No. 6, pp. 74–79, June, 2015. Original article submitted March 6, 2015.

The aim of the present work is to investigate the microstructure, chemical composition, and nanohardness of the layers of the solid-state titanium alloy – nickel – stainless steel joint to detect regions of crack nucleation and to determine ways for further improvement of the joint hardness.

EXPERIMENTAL

Specimens of the PT-3V titanium alloy and Fe–12Cr–18Ni–10Ti steel with sizes of $4 \times 4 \times 20$ mm^3 were joined through the NP-2 nickel interlayer with a thickness of 0.3 mm in a vacuum furnace with residual gas pressure not higher than $P = 2.0 \cdot 10^{-3}$ Pa. The welding regime was the following: pressure $P = 4$ MPa, temperature $T = 600$, 700, and 750°C, and time of holding under pressure $\tau = 20$ min. After welding the specimens were annealed at welding temperatures for 1 h. To investigate the mechanical properties at room temperature, the specimens were subjected to tensile tests with the strain rate $\dot{\varepsilon} = 2 \cdot 10^{-3}$ s^{-1}. To facilitate investigation of the joint zones, oblique microsections with the cutting angle $\alpha = 10°$ to the joint surface were cut on an electrospark machine. The microsections were successively polished with diamond pastes having different grain sizes and then with colloid silicon dioxide suspensions having particle sizes of about 0.04 μm. Some microsections were subjected to electrochemical etching in the solution of 200 mL butanol and 20 mL $HClO_4$. The microstructure was investigated using a 6610LV scanning microscope with an INCA energy dispersive spectrometer. The hardness of the joint zone was determined by impact indentation using a Nanoskan 3D nanoindenter. The scanning resolution was about 10 nm in the *XY* plane and no worse than 1 nm along the *Z* axis. As a tip, the Berkovich diamond indenter was used shaped as a triangular pyramid with a tip angle of 140° and the tip curvature radius $r \approx 50$ nm. The load applied to the indenter was $P = 20$–30 mN.

RESULTS

As a result of joining, a layered composite was formed in which two interfaces can be distinguished: between the titanium alloy and nickel and between the stainless steel and nickel. The titanium alloy – nickel joint zone consists, in turn, of several layers (Fig. 1*a* and *b*). The formation of three kinks corresponding to Ti_2Ni, TiNi, and $TiNi_3$ intermetallic compounds can be seen in the dependence of the composition on the distance. The TiNi and $TiNi_3$ kinks were formed in the specimen at $T = 650$°C, whereas the layer with the Ti_2Ni stoichiometry was not observed; however, the region of changed microstructural state existed between Ti and TiNi. In this region of the titanium alloy the nickel content was high. At $T = 750$°C, the kinks were more clearly pronounced and were wider than after welding at $T = 700$°C. The intermediate zones between the kinks corresponded to the two-phase regions. The width of the titanium alloy – nickel joint zone in which the intermetallic layers were formed was 8–10 and 12–14 μm at $T = 700$ and 750°C, respectively. A comparison of the etched and non-etched microsections allowed a curious fact to be revealed. The polished microsections looked continuous, whereas periodic small cracks were observed on the etched microsections. The microcracks were observed in two layers: Ti_2Ni and $TiNi_3$. No cracks were observed in the TiNi layer.

The nickel – stainless steel joint zone had no continuous layered structure analogous to that of the titanium alloy – nickel zone. Small particles with sizes smaller than 1 μm enriched with chromium were present in this zone (Fig. 2). The width of the nickel – stainless steel joint zone was equal to 15–20 μm. It depended weakly on the weld temperature.

The nanohardness measured in the titanium alloy – nickel joint zone is shown in Fig. 3. The hardness changed non-uniformly in the region of the Ti–Ni intermetallic compound. Zones with high hardness altered with low hardness zones. Ti_2Ni and $TiNi_3$ layers had the highest hardness.

The fractograms of specimens fractured in tensile tests at 20°C demonstrated that failure was inhomogeneous and two zones were distinguished in the specimen: the central part and the edge. The inhomogeneity of failure was due to the formation of a stagnant zone in the central part of the specimen being welded that was caused by a strong increase in the friction coefficients of the surfaces being welded and their subsequent sticking. The following regularity was found for all examined weld temperatures: the central parts of the specimens failed along the Ti + Ti_2Ni/TiNi interface, whereas at the edge of the specimens, they failed along the TiNi/$TiNi_3$ interface. When the weld temperature *T*

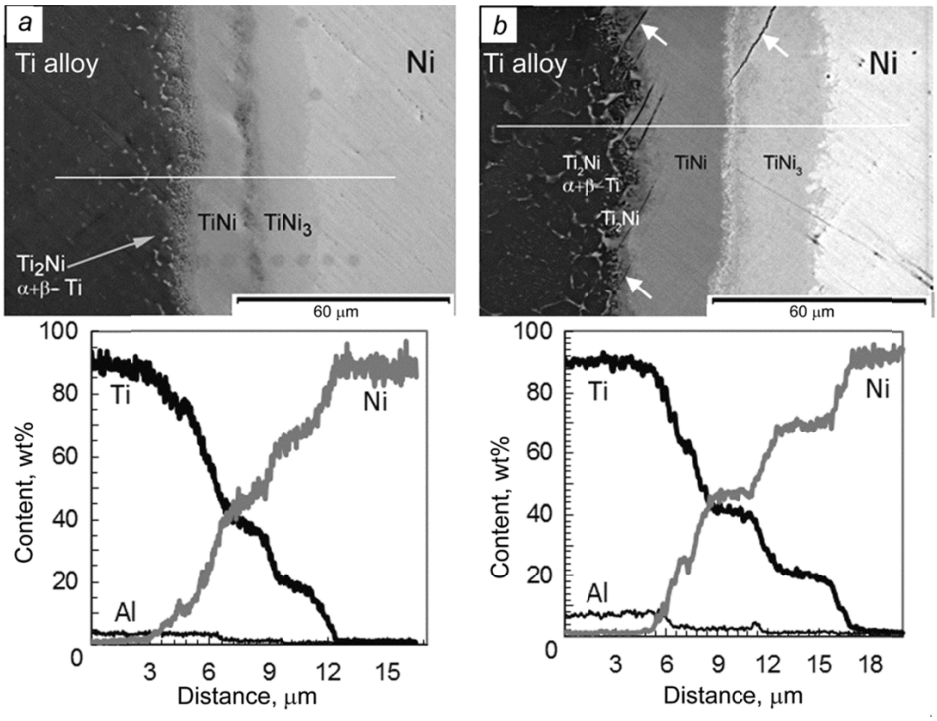

Fig. 1. Titanium alloy – nickel joint zone after welding at temperatures $T = 700$ (*a*) and 750°C (*b*). The microsections were preliminary etched. The secondary electron image is shown. The arrows indicate cracks in the Ti_2Ni and $TiNi_3$ layers.

increased from 650 to 750°C, the relative contribution of the central part of the failure to the entire failure area of the specimen decreased from 56 to 45%.

The temperature of pressure welding affects the chemical composition of the central part of the failure. At $T = 650$°C the central part of the fractured specimen comprised 5–10 wt% Ni, which corresponded to the mixture of titanium alloyed by nickel and the Ti_2Ni phase. With increasing weld temperature, the Ti content decreased, and the composition of the central part of the failure approached to that of stoichiometric Ti_2Ni. The composition of the edge zone depended weakly on the weld temperature. This is due to the fact that Ti_2Ni and $TiNi_3$ layers whose composition is close to the stoichiometric one were formed already at $T = 650$°C, and with further increase in the weld temperature, only their thickness increased. Figure 4 shows two failure surfaces of the specimen obtained by pressure welding at the temperature $T = 750$°C and fractured at $T = 20$°C. In the central part, it fractured along the Ti_2Ni/TiNi interface. At the edges of the specimen, the fracture was mixed in character, and the specimen failed mainly along the TiNi/$TiNi_3$ interface; however, fracture islets were also observed in the $TiNi_3$ phase (they are indicated by arrows).

DISCUSSION

It is obvious that the reason for the specimen fracture at $T = 20$°C is the network of microcracks arising in the Ti_2Ni and $TiNi_3$ layers upon cooling. Let us analyze the reasons for the formation of such network of microcracks. The literature contains little information about the Ti_2Ni and $TiNi_3$ phases. $TiNi_3$ has the hexagonal closely packet (HCP) lattice of DO24 type characterized by the limited number of slip systems and low ductility [6, 7]. The Ti_2Ni phase has E93 cubic structure and is also brittle. The data on the TECs of $TiNi_3$ and Ti_2Ni are lacking in the literature. However, the TECs of the $TiNi_3$ and Ti_2Ni phases can be estimated roughly from the empirical dependence of the TEC on the melt temperature T_{melt} (the Lindemann criterion) [8]:

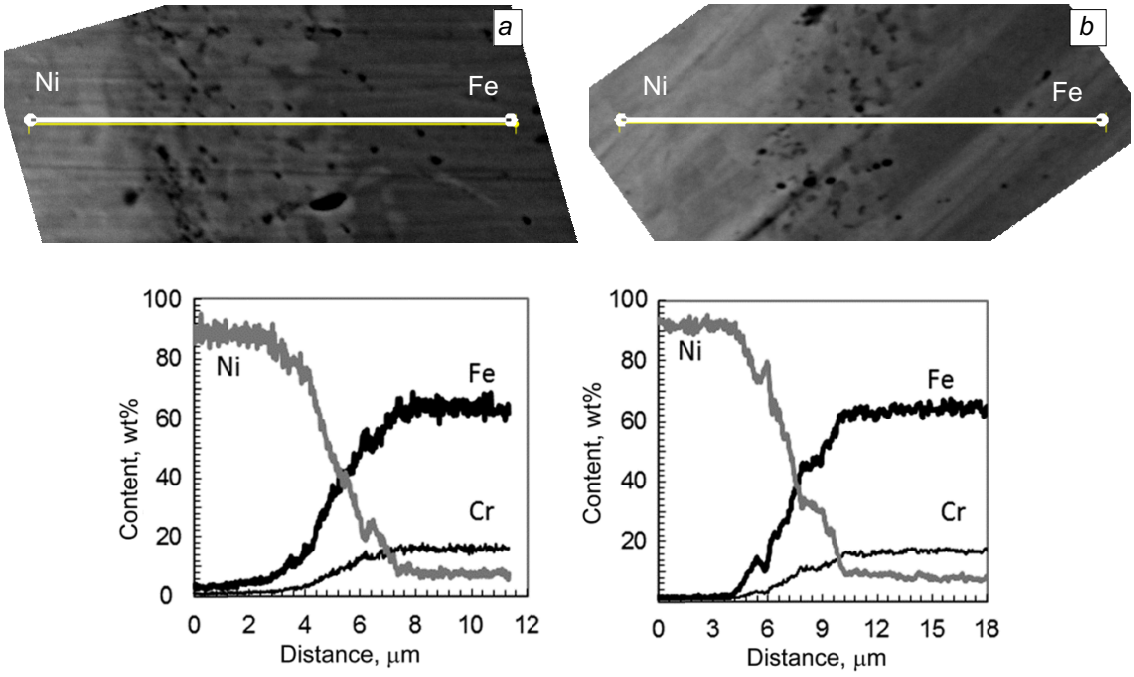

Fig. 2. Nickel – stainless steel joint zone after welding at temperatures $T = 700$ (*a*) and 750°C (*b*). Microsections were preliminary etched. The secondary-electron image is shown.

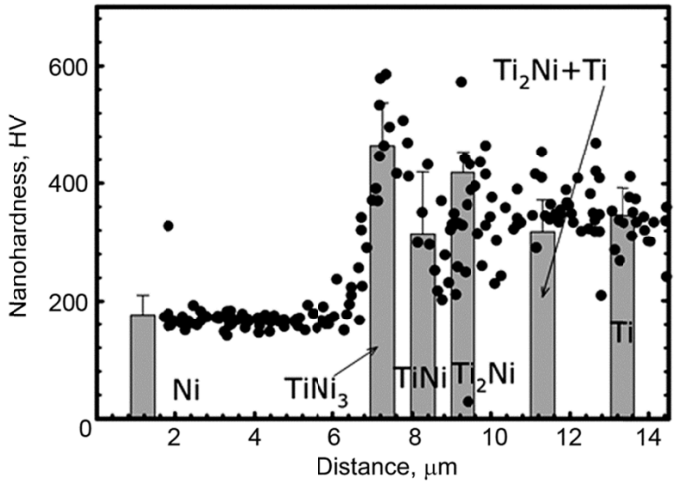

Fig. 3. Change in the nanohardness of the titanium alloy – nickel joint zone after welding at $T = 750$°C.

$$\alpha T_{\text{melt}}^{n} = A, \tag{1}$$

where α is the TEC and n and A are constants. For substances with metallic bonds, $n = 1.17$ and $A = 7.24 \cdot 10^{-2}$. From Eq. (1) it follows that the TEC of solids is the higher, the lower is their melting temperature. Our estimate demonstrates that the most probable intervals of TEC variations for the $TiNi_3$ and Ti_2Ni phases at room temperature are

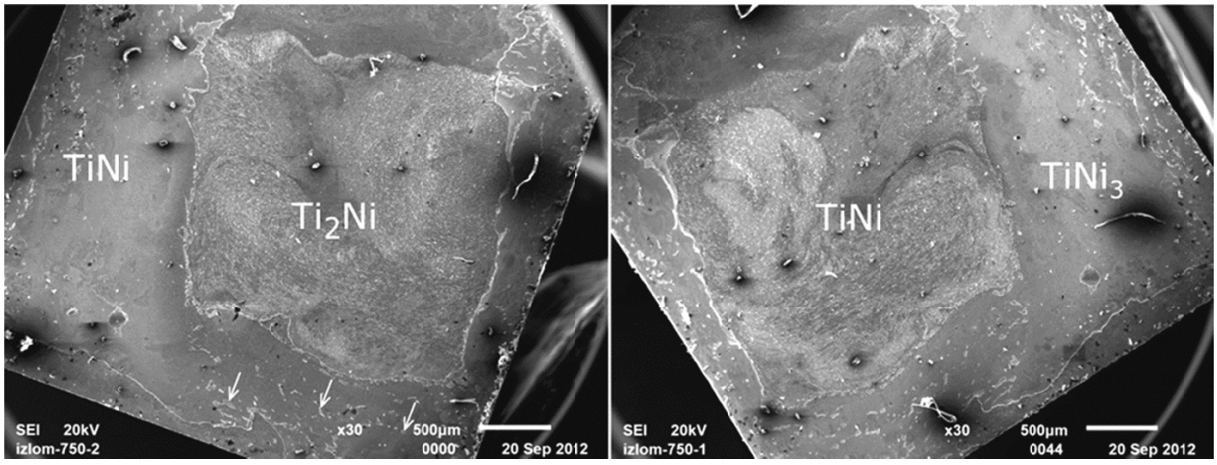

Fig. 4. Two failure surfaces of the specimen obtained by high pressure welding at $T = 750$°C and fractured in tensile tests at room temperature. The arrows indicate particles of the $TiNi_3$ phase.

$(12 \pm 2)\cdot10^{-6}$ °C^{-1} and $(16 \pm 2)\cdot10^{-6}$ °C^{-1}, respectively. The Ti_2Ni phase is in contact with Ti, and its TEC is almost doubled compared with the TEC of titanium ($\alpha = 8.6\cdot10^{-6}$ °C^{-1} for Ti). Therefore, upon cooling of the Ti/Ti_2Ni contact zone, the Ti_2Ni phase will be subjected to tensile stresses. The $TiNi_3$ phase is in contact with Ni, and their TECs almost coincide ($\alpha = 13\cdot10^{-6}$ °C^{-1} for Ni). Therefore, no significant stresses will be observed at the $TiNi_3$/Ni interface upon cooling.

Another situation takes place at the interfaces of TiNi with Ti_2Ni and $TiNi_3$. It is well known that the TiNi phase possesses the shape memory effect and is ductile. The reversible austenitic-martensitic transformation in TiNi occurs at temperatures $T = 20$–100°C depending on the nickel content. For example, a change in the nickel content by 0.1 at.% changes the transformation temperature by about 10°C. The TiNi ductility can reach several percent [9]. The TEC of the TiNi phase changes during transformation from austenitic (CsCl cubic structure of *B*2 type) to martensitic one (monoclinic structure of *B*19' type). Far from the interval of the phase transformation temperature, the martensitic TEC is $6.6\cdot10^{-6}$ °C^{-1}, whereas the austenitic TEC is $11\cdot10^{-6}$ °C^{-1}. However, at the moment of the austenitic–martensitic or austenitic–rhombohedral *R*-phase transition (in the temperature interval 20–100°C for equiatomic compositions), the TEC changes anomalously strongly [10]. In the narrow temperature interval (about 20°C), the austenitic–martensitic transformation is accompanied by the TEC jump to $-30\cdot10^{-6}$ °C^{-1}. If the transformation goes through the *R*-phase, the TEC of the material can reach $+120\cdot10^{-6}$ °C^{-1} or have a sign-variable value of $\pm60\cdot10^{-6}$ °C^{-1} depending on the dislocation density. It can be seen that the change in the TEC during phase transformation in TiNi greatly exceeds the difference of the TECs between other pairs of layers. Therefore, this suggests that exactly the phase transformation in the TiNi layer is the main reason for the formation of the microcrack network in the adjacent Ti_2Ni and $TiNi_3$ layers.

CONCLUSIONS

1. Joining of the titanium alloy and the stainless steel through the nickel interlayer at temperatures $T = 650$, 700, and 750°C is accompanied by the formation between the titanium alloy and nickel of continuous Ti_2Ni, TiNi, and $TiNi_3$ layers of intermetallic compounds separated by two-phase regions. The nickel – stainless steel joint zone has no continuous layered structure. The intermetallic compounds in it are distinguished as individual particles enriched with chromium and having sizes smaller than 1 μm.

2. In the region of intermetallic compounds between the titanium alloy and nickel, the hardness changes extremely non-uniformly: zones with increased and decreased hardness follow one another. The Ti_2Ni and $TiNi_3$ layers have the highest hardness.

3. The uniformly distributed microcracks were detected in the Ti_2Ni and $TiNi_3$ layers after joining at temperatures exceeding $T = 700°C$, whereas they were not observed in the TiNi layer. Microcracks appeared under cooling of specimens from the weld temperature. It seems likely that cracking is initiated by the anomalously large change of the linear thermal expansion coefficient during the austenitic–martensitic transformation in the TiNi layer.

4. During mechanical tests at $T = 20°C$, the specimens always fractured in the joint between the titanium alloy and nickel. Wherein, the fracture surface in the central part and at the edge of the specimens was observed in different layers of the material. In the central part of the specimens, they fractured mainly along the Ti_2Ni/TiNi interface, whereas at the edges they fractured along the TiNi/$TiNi_3$ interface.

REFERENCES

1. S. Kundu and S. Chatterjee, Mater. Characteriz, **59**, 631–637 (2008).
2. R. G. Budinsky, Wear, **151**, 203–217 (1991).
3. M. Ferrante and E. V. Pigoretti, J. Mater. Sci., **37**, 2825–2833 (2002).
4. R. G. Khazgaliev, M. Kh. Mukhametrakhimov, R. R. Mulyukov, and R. Ya. Lutfullin, Perspekt. Mater., **12**, 529–534 (2011).
5. S. Kundu, S. Chatterjee, D. Olson, and B. Mishra, Metallurg. Mater. Trans., **A38**, 2053–2060 (2007).
6. J. L. C. Daams, Atlas of Crystal Structure Types for Intermetallic Phases, ASM International, Newbury (1991).
7. M. H. Mueller and H. W. Knott, Trans. AIME, **227**, 674–678 (1963).
8. S. I. Novikova, Thermal Expansion of Solid Bodies [in Russian], Nauka, Moscow (1974).
9. V. N. Khachin, V. G. Pushin, and V. V. Kondrat'ev, Titanium Nickelide: Structure and Properties [in Russian], Nauka, Moscow (1992).
10. J. Uchil, K. P. Mohanchandra, K. Ganesh Kumara, *et al*., Physica, **B270**, 289–297 (1999).